International Journal of Coal Geology 162 (2016) 14–26

Contents lists available at ScienceDirect

International Journal of Coal Geology

journal homepage: www.elsevier.com/locate/ijcoalgeo

Hydrogeochemistry and coal-associated bacterial populations from a methanogenic coal bed

Elliott P. Barnhart [a,f,g,*], Edwin P. Weeks [b], Elizabeth J.P. Jones [c], Daniel J. Ritter [d], Jennifer C. McIntosh [d], Arthur C. Clark [e], Leslie F. Ruppert [c], Alfred B. Cunningham [f,h], David S. Vinson [i], William Orem [c], Matthew W. Fields [f,g,j]

[a] U.S. Geological Survey, 3162 Bozeman Ave, Helena, MT 59601, United States
[b] U.S. Geological Survey, National Research Program, Denver Federal Center, Lakewood, CO 80225, United States
[c] US Geological Survey, 12201 Sunrise Valley Drive, Reston, VA 20192, United States
[d] Department of Hydrology and Water Resources, University of Arizona, Tucson, AZ 85721, United States
[e] U.S. Geological Survey, Denver Federal Center, Lakewood, CO 80225, United States
[f] Center for Biofilm Engineering, Montana State University, Bozeman, MT 59717, United States
[g] Department of Microbiology and Immunology, Montana State University, Bozeman, MT, 59717, United States
[h] Department of Civil Engineering, Montana State University, Bozeman, MT, 59717, United States
[i] Department of Geography & Earth Sciences, University of North Carolina at Charlotte, Charlotte, NC, 28223, United States
[j] National Center for Genome Resources, Santa Fe, NM, 87505, United States

ARTICLE INFO

Article history:
Received 8 January 2016
Received in revised form 1 May 2016
Accepted 2 May 2016
Available online 4 May 2016

Keywords:
Powder River Basin
Coalbed methane
Microbial enhanced CBM (MECoM) technology
Test site
Biosurfactant
Hydrology
Hydrogeochemistry

ABSTRACT

Biogenic coalbed methane (CBM), a microbially-generated source of natural gas trapped within coal beds, is an important energy resource in many countries. Specific bacterial populations and enzymes involved in coal degradation, the potential rate-limiting step of CBM formation, are relatively unknown. The U.S. Geological Survey (USGS) has established a field site, (Birney test site), in an undeveloped area of the Powder River Basin (PRB), with four wells completed in the Flowers-Goodale coal bed, one in the overlying sandstone formation, and four in overlying and underlying coal beds (Knoblach, Nance, and Terret). The nine wells were positioned to characterize the hydraulic conductivity of the Flowers-Goodale coal bed and were selectively cored to investigate the hydrogeochemistry and microbiology associated with CBM production at the Birney test site. Aquifer-test results indicated the Flowers-Goodale coal bed, in a zone from about 112 to 120 m below land surface at the test site, had very low hydraulic conductivity (0.005 m/d) compared to other PRB coal beds examined. Consistent with microbial methanogenesis, groundwater in the coal bed and overlying sandstone contain dissolved methane (46 mg/L average) with low $\delta^{13}C$ values (−67‰ average), high alkalinity values (22 meq/kg average), relatively positive $\delta^{13}C$-DIC values (4‰ average), and no detectable higher chain hydrocarbons, NO_3^-, or SO_4^{2-}. Bioassay methane production was greatest at the upper interface of the Flowers-Goodale coal bed near the overlying sandstone. Pyrotag analysis identified *Aeribacillus* as a dominant *in situ* bacterial community member in the coal near the sandstone and statistical analysis indicated *Actinobacteria* predominated coal core samples compared to claystone or sandstone cores. These bacteria, which previously have been correlated with hydrocarbon-containing environments such as oil reservoirs, have demonstrated the ability to produce biosurfactants to break down hydrocarbons. Identifying microorganisms involved in coal degradation and the hydrogeochemical conditions that promote their activity is crucial to understanding and improving *in situ* CBM production.

1. Introduction

1.1. Biogenic coal bed methane

Biogenic coalbed methane (CBM) has become an important natural gas resource in the United States, Canada, Australia, India, and China (Palmer, 2010). Accumulation of CBM in deep coal beds is primarily a by-product of thermal coalification processes, while in shallower coal beds, such as those in the Powder River Basin (PRB) in southeastern Montana and northeastern Wyoming, biogenic CBM accumulates from the activity of *in situ* microbial communities (Barnhart et al., 2013; Faiz and Hendry, 2006; Ritter et al., 2015; Strąpoć et al., 2011). The microbial communities in the PRB have produced an estimated 14.26 trillion cubic feet (TCF) of biogenic CBM that has been developed commercially over the past few decades (Strąpoć et al., 2011; U.S.

* Corresponding author at: USGS Wyoming-Montana Water Science Center, 3162 Bozeman Ave., Helena, MT 59601, United States.

http://dx.doi.org/10.1016/j.coal.2016.05.001

Geological Survey National Assessment of Oil and Gas Resources Team et al., 2014). There were approximately 17,500 active CBM production wells in the PRB in 2008, but production was short-lived with an average productive well life of <12 years (Meredith et al., 2012; Sando et al., 2014). Push-pull tests indicate the microbial communities within PRB coal beds are active and have generated biogenic CBM in the recent geologic past (Ulrich and Bower, 2008). Several hypothetical models for active microbial CBM formation have been proposed that involve the anaerobic degradation of coal by bacteria, which results in the formation of precursor metabolites that cross-feed methane-producing archaea (methanogens) (Jones et al., 2010; Meslé et al., 2013; Strąpoć et al., 2008). The rate-limiting step of microbial CBM formation appears to be the initial bacterial degradation of coal organic matter constituents (Wawrik et al., 2011). Currently, neither the specific bacterial communities and enzymes nor the optimal *in situ* conditions for bacterial coal degradation are known.

Increasing coal bioavailability and/or stimulating specific bacterial populations involved in coal degradation with microbial enhanced CBM (MECoM) technology could increase *in situ* CBM production and sustain the life of wells in the PRB and other basins. Private companies have implemented pilot scale MECoM tests in the PRB, but have not been able to predict or document the associated changes to the bacterial community, partly due to the current lack of understanding of the *in situ* bacterial community dynamics within the coal beds (Ritter et al., 2015). Recent advances in DNA sequencing technology coupled with improved sampling of the subsurface matrix have allowed for better characterization of microbial communities in environmental samples (Barnhart et al., 2013). Next-generation sequencing provides the coverage required to establish correlations between the microbial community composition and environmental conditions that drive the microbial community dynamics. These techniques were utilized in this study along with a multidisciplinary approach to investigate the hydrogeochemical characteristics of several major PRB coal beds along a vertical transect.

1.2. Microbial CBM formation in the PRB

The PRB contains one of the most significant, low-rank (subbituminous) coal deposits in the world (Molnia and Pierce, 1992). Low-rank coals are thought to contain a higher proportion of bioavailable compounds and macerals richer in heteroatoms than higher-rank coals (Strąpoć et al., 2011). Production of CBM from the PRB mostly occurs from coal beds in the Paleocene Tongue River Member of the Fort Union Formation (Fig. 1) (Ellis et al., 2002; Flores et al., 2008; Rice et al., 2008; Scott et al., 2011). Several coal beds in the Tongue River Member, which are investigated here, include the Knobloch, Nance, Flowers-Goodale, and Terret coal beds (Fig. 2). It has been suggested that groundwater recharge originally inoculated these and other PRB coal beds with the active CBM-producing microbial communities (Strąpoć et al., 2011). Shallow groundwater in recharge areas of these coal beds, which commonly contains sulfate, has low methane concentrations. Sulfate-reducing bacteria can outcompete methane-producing methanogens for substrates (Meredith et al., 2012; Raskin et al., 1996). As groundwater moves deeper in the coal beds, bacterially-mediated sulfate reduction lowers the aqueous sulfate levels and increases the bicarbonate concentrations so methanogenesis may proceed (Brinck et al., 2008).

Microbial methanogenesis in the PRB is identifiable by distinctive gas and groundwater geochemical signatures. PRB gas is dry (very low in ethane or $\geq C_3$ hydrocarbons) and exhibits fairly negative $\delta^{13}C\text{-}CH_4$ values typical of microbial gas (−83‰ to −51‰; Bates et al., 2011; Flores et al., 2008; Gorody, 1999). The isotope fractionation that generates negative $\delta^{13}C\text{-}CH_4$ values also yields positive values of $\delta^{13}C\text{-}CO_2$. Biodegradation that includes sulfate reduction and methanogenesis generates CO_2, although with different (opposite) isotopic values for sulfate reduction and methanogenesis, respectively. The $\delta^{13}C\text{-}CO_2$ values for sulfate reduction tend to be lower, closer to the value of organic matter (coal), while $\delta^{13}C\text{-}CO_2$ values for methanogenesis become increasingly more positive with greater extents of methanogenesis (Osborn and McIntosh, 2010). The $\delta^{13}C\text{-}CO_2$ values of producing gas wells in the PRB range from −25‰ to 22‰ (‰; Bates et al., 2011; Flores et al., 2008; Gorody, 1999). Due to microbial respiration, PRB coal bed groundwater exhibits high alkalinity concentrations (6–50 meq/kg; Bates et al., 2011).

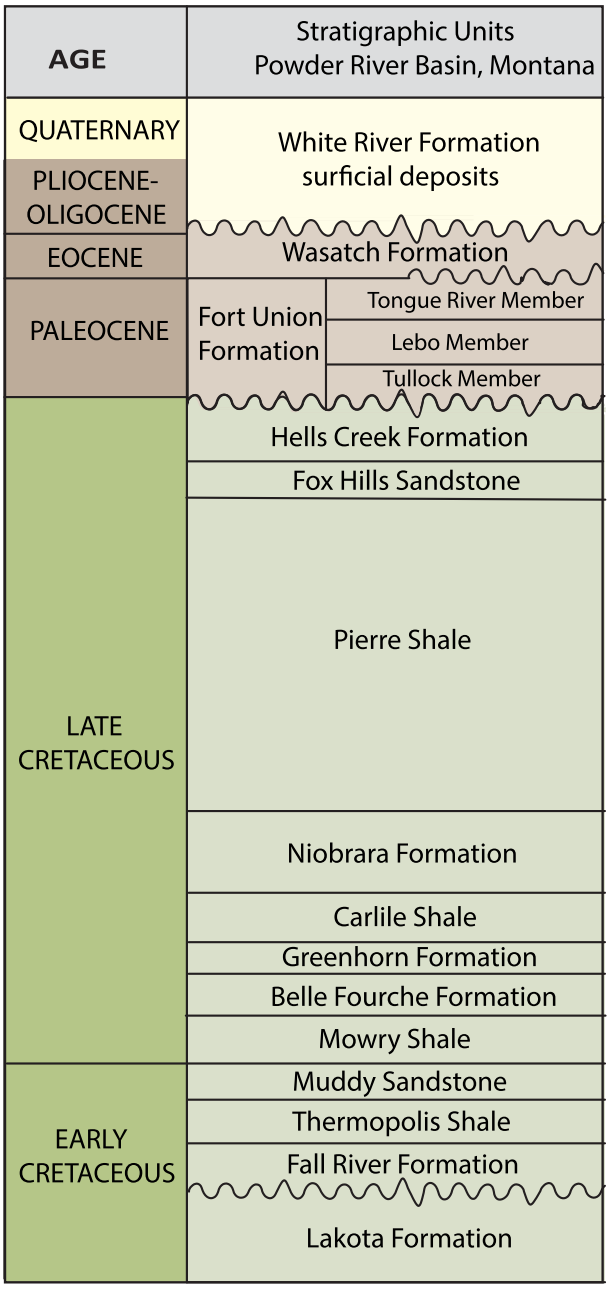

Fig. 1. Generalized stratigraphic column of the Montana part of the Powder River Basin. Coal beds examined in this study occur in the Paleocene Fort Union Formation, Tongue River Member. (Modified from Scott et al., 2011, after Ellis et al., 2002).

Regionally, groundwater in the PRB is believed to move northward to northeastward but the relative importance (or contribution) of regional versus local flow systems and vertical versus horizontal flow components are not well understood (Bates et al., 2011; Rice et al., 2008). Understanding the flow velocity and direction can help interpret the extent of methanogenesis and the environment within which methanogenesis occurs. A carefully designed aquifer test with specific well placement and sophisticated analytical techniques can be used to determine local groundwater flow and hydraulic conductivity within a

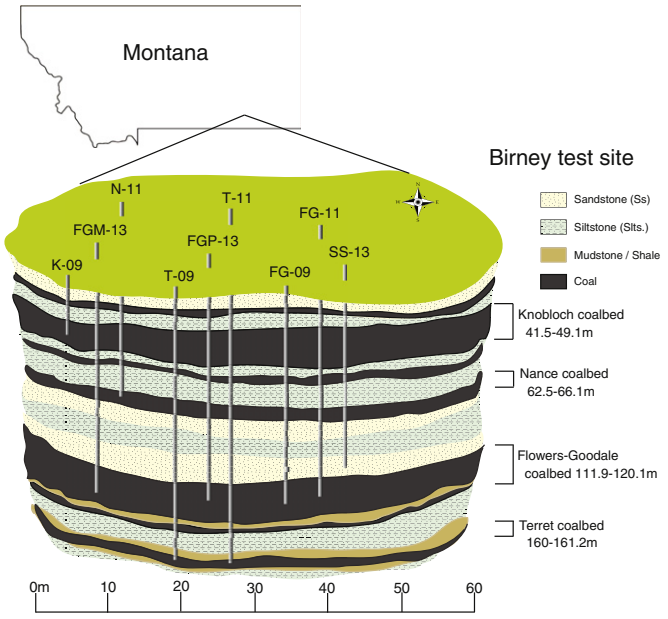

Fig. 2. Birney test site consists of nine wells that access four major PRB coal seams (Knobloch (K), Nance (N), Flowers-Goodale (FG), and Terret (T)). Water samples were collected for geochemistry analysis and cores were obtained from T-11 and FG-11 for further geochemistry and microbiology analysis.

coal bed (Weeks, 2005). Coal beds function as complex aquifers resulting from their typical cleat (fracture) structure, consisting of extensive face cleats intersected at approximate right angles by butt cleats, which end at face cleats. This structure results in anisotropic transmissivity, with the major transmissivity axis being parallel to the face cleat direction. Coal also represents a dual-porosity medium, with flow occurring not only through the cleat network, but with the coal matrix blocks supplying an added storage mechanism that slowly exchanges water with the cleats as cleat pressure changes. Cleats and cleat interfaces provide a larger area for microbial colonization than mesopores and macropores (which can range from 0.04 to 30 μm within the matrix of low-rank coals) (Bale et al., 1984; Rouquerolt et al., 1994).

Molecular techniques have been applied to investigate the bacterial and archaeal communities present in PRB coal beds via SSU rRNA gene sequences (Barnhart et al., 2013; Jones et al., 2013; Klein et al., 2008). These studies indicate that the *in situ* bacterial community is much more diverse than the archaeal community, and the bacterial communities are often dominated by bacteria in the *Proteobacteria, Firmicutes*, and *Actinobacteria* phyla (Ritter et al., 2015). Filamentous microorganisms, such as *Actinobacteria*, can potentially penetrate the smaller pores within the coal matrix with filaments supported by turgor pressure, which could provide an advantage for these microorganisms (Faison, 1992). In addition, certain *Actinobacteria* have demonstrated the ability to produce biosurfactants that can break down hydrocarbons and facilitate the uptake of difficult-to-access carbon sources in subsurface environments (Kügler et al., 2015). A vertical profile of microbial communities through a coal bed has not been explored in the literature because many studies have been limited to small datasets, typically obtained from a single coal sample or from pumped groundwater that does not reflect the microbial densities and activities in the subsurface (Alfreider et al., 1997; Klein et al., 2008; Wawrik et al., 2011).

The U.S. Geological Survey (USGS) established a field site, the Birney test site, in an undeveloped area of the PRB with nine wells that are completed in four PRB coal beds (Knobloch, Nance, Flowers-Goodale, and Terret coal beds) as well as an overlying sandstone formation (Fig. 2) to obtain significant core and water samples to better understand the hydrogeochemical conditions and microbial communities responsible for biogenic CBM formation. The site was established with an end goal to understand, effectively implement, and monitor MECoM technology. The wells were installed and selectively cored to initially assess the hydrogeochemical conditions associated with CBM production and further study the bacterial diversity within and around a methane-containing coal bed. The Birney test site has multiple wells screened in the same coal bed (Flowers-Goodale) for the determination of hydraulic properties, flow direction, and flow velocity to document natural conditions which constrain CBM production and future MECoM stimulation efforts. A bioassay of coal core samples vertically through the Flowers-Goodale coal bed indicated areas of increased bioavailability within the coal bed. DNA sequences indicative of *Actinobacteria* and *Aeribacillus* predominated areas of increased coal bioavailability within the coal bed. This analysis allowed new insight into potential *in situ* bacterial populations involved in coal degradation and the hydrogeochemical conditions that promote CBM formation.

2. Methods and materials

2.1. Field site location and description

The selected field test site (the Birney test site) is in the PRB in Rosebud County near Birney, Montana on land administered by the Bureau of Land Management. Initial site characterization involved drilling three exploratory test holes, which encountered six coal beds within 170 m of land surface, including, with increasing depth, the Sawyer, Knobloch, Calvert, Nance, Flowers-Goodale, and Terret coals. The Knobloch, Nance, Flowers-Goodale and Terret coal beds were cored and desorbed to measure gas content and composition (Table 1). The Knobloch and Nance contained no gas while the Flowers-Goodale and Terret coals did contain gas. Based on this information, the decision was made to further investigate (*i.e.* set monitor wells and collect water-quality data) the Knobloch, from 41.5 to 49.1 m in depth, the Flowers-Goodale, from 111.9 to 120.1 m in depth, and the Terret, from 160 to 161.2 m in depth (Fig. 2). Initial observation wells were installed tapping each of these coals, including K-09 (Knobloch), screened from 45.7 to 48.8 m, FG-09 (Flowers-Goodale), screened from 114.9 to 118.0 m depth, and T-09 (Terret), screened from 159.4 to 162.5 m. Three additional wells were installed in 2011, including one in the Nance coal bed, from 62.5 to 66.1 m depth (N-11), an additional well in the Flowers-Goodale (FG-11), and a second well in the Terret (T11). Cores from wells T-11 and FG-11 are discussed in this paper (Fig. S1).

Aquifer tests performed even on well-confined coal beds require carefully designed observation well placement and sophisticated analytical techniques for successful interpretation (Weeks, 2005). Based on these concepts, two additional wells in the Flowers-Goodale coal (FGP-13 and FGM-13) were drilled in 2013, to provide a total of four wells tapping the Flowers-Goodale coal. The layout for the four wells include the planned production well, FGP-13, surrounded by three approximately equally spaced observation wells (FGM13, FG-09, and FG-11), separated at approximately 120° angles. This layout was chosen to allow identification of the magnitude and bearing of the anisotropic

Table 1
Gas desorption data for selected intervals of the Knobloch, Nance, Flowers-Goodale, and Terret coal beds. Reported gas content includes both desorbed and residual gas in standard cubic feet per ton (scf/ton) and standard cubic centimeters per gram (scm3/g) of coal.

Core	Coal bed	Depth (m)	Total gas content (scf/ton)	Total gas content (scm3/g)
T-11	Knobloch	41.94–42.31	0	0
T-11	Knobloch	44.17–44.47	0	0
T-11	Knobloch	47.24–47.85	0	0
T-11	Nance	63.09–63.40	0	0
T-11	Flowers-Goodale	112.62–112.93	16.7	0.52
T-11	Flowers-Goodale	113.81–114.12	17.24	0.54
T-11	Flowers-Goodale	115.83–116.44	19.21	0.6
T-11	Flowers-Goodale	117.65–117.96	16.64	0.52
T-11	Terret	163.22–163.83	11.21	0.35

transmissivity tensor representing the Flowers-Goodale coal. In addition, an observation well tapping the sandstone overlying the coal (SS-13) was installed to monitor effects of leakage from the coal. Overall well placement and generalized stratigraphy of the Birney field site is shown in Fig. 2, and specific well construction details for the Birney test site can be found in Table S1.

2.2. Field handling/sample collection

Core samples from T-11 and FG-11 were extruded into a wooden trough and wiped clean to remove drilling fluids from the outside of the core samples. The geology and corresponding depth from the core samples are described in Figure S1. Samples for methane desorption analysis were collected from the Knobloch, Nance, Flowers-Goodale and Terret coal seams (Table 2). Desorbed gas samples were collected in Tedlar bags from Isotech Laboratories, Inc. attached directly to polyvinyl chloride (PVC) desorption canisters. Bags were shipped to Isotech Laboratories for analysis of gas isotopes and gas composition. Several samples from each coal zone also were selected for ultimate and proximate analysis to determine the coal's energy value and composition. Solids were collected from intervals directly above, within, and directly below the Flowers-Goodale coal section in T-11 and FG-11 for microbial analysis (Fig. S1). Samples from these intervals of the core section were transferred to a disposable glove bag filled with N_2, exposed outer core was removed, and coal was sampled using sterile implements. Samples for DNA analysis were immediately frozen on dry ice and transported to a −80 °C freezer at Montana State University.

2.3. Water and dissolved gas sampling

Water-quality samples were collected after wells had been pumped for sufficient time to purge 3 well volumes of water from the well. All water samples were filtered through a 0.45-μm nylon filter and stored on ice or in the lab at 4 °C until analysis. Alkalinity was titrated within 12 h of sample collection using the Gran-Alkalinity titration method (Gieskes and Rogers, 1973). Samples for major ions were collected in 60-mL high-density polyethylene (HDPE) bottles with no headspace, and concentrated nitric acid was added to cation samples for preservation (pH < 2). Samples for δ^{13}C-DIC were collected in glass serum bottles, preserved with mercuric chloride, and capped with no headspace.

Subsamples for dissolved organic carbon (DOC) and volatile fatty acids (VFAs) were filtered using a clean glass syringe and Whatman Polyethersulfone (PES) 0.2-μm syringe filters into clean amber glass vials for DOC and plastic scintillation vials for VFAs. VFA samples were frozen on dry ice to prevent biodegradation, and DOC samples were kept cool on water ice in the field and later refrigerated in the lab until analysis (generally within one week). Glassware and glass bottles were precleaned either by baking in a furnace (450 °C for 2 h) or by washing with dichloromethane (DCM) (Orem et al., 2007). Field blanks, consisting of MilliQ water taken into the field in clean glass bottles and processed in the same manner as produced water samples, were used to assess any contamination from sample handling or processing. Field blanks consistently showed little or no contamination. DOC values reflected that of pure MilliQ water, VFAs were not detected, and extractable hydrocarbons consisted of little other than small peaks for phthalates.

Detailed analytical procedures have been previously described (Orem et al., 2014). Briefly, DOC was determined using a Shimadzu TOC-VCPH analyzer equipped with a catalytically-aided 680 °C combustion chamber and normal sensitivity catalyst. Standardization for DOC was based on a 5-point calibration curve using an aqueous potassium phthalate standard (100 ppm, or 10 ppm depending on the DOC range of the samples). The detection limit is approximately 0.3 ppm. ASTM Type I Reagent Water was used as an analytical blank, and each sample was analyzed at least four times to ensure data consistency. Percentage relative standard deviation (%RSD) for DOC analysis is <10%. VFAs were analyzed using high-performance liquid chromatography (HPLC) with a Waters Corporation Alliance HT autosampler and 996 photodiode array detector, and an Alltech Prevail organic acid column (150mm × 4.6 mm; 5 μm packing). A solution of KH_2PO_4 (25 mmol L^{-1}, pH 2.5) was used as eluent, with a flow rate of 1.5 mL min^{-1}. Chromatograms were extracted from the diode array spectrum at 205 nm. Standard solutions were prepared from serial dilutions of 2000 mg L^{-1} stock standards of pure fatty acids (C_1–C_4) in MilliQ water. The detection limit ranged from 0.1 to 1 mg L^{-1}, depending on the complexity of the sample matrix; values <1 mg L^{-1} are considered semi-quantitative. Samples were analyzed at least in duplicate and %RSD is usually <10%.

Major ion concentrations were analyzed at the University of Arizona Department of Hydrology and Water Resources. Major cations were analyzed with a Perkin-Elmer Optima 5100DV Inductively Coupled Plasma-Optical Emission Spectrometer (precision ±2%). Major anions were analyzed using a Dionex Ion Chromatograph model 3000 with an AS23 analytical column (precision ±2%). Charge balance error was <5% for all measured waters.

Dissolved gas samples were collected using dissolved gas bottles and IsoFlasks from Isotech Laboratories, Inc. For all sampling campaigns (2009–2014), dissolved gas bottles were used to collect samples. In the summer of 2014, IsoFlasks also were used to collect samples from wells in the Terret and Flowers-Goodale coal seams. When dissolved gas bottles were used, samples for gas isotopes and gas composition were collected by filling a 5-gallon bucket with water. Next, the bottle was submerged and inverted. A hose from the well was then inserted into the bottle, and water and gas were allowed to flow into the bottle for approximately 5 min. The hose was removed, and the bottle was capped upside down and stored inverted on ice until it was sent to Isotech Laboratories for analysis. In addition, in order to measure dissolved methane concentration, a second bottle was filled in a similar manner, but with the submerged bottle remaining upright instead of inverted. When IsoFlasks were used (summer 2014), a special fill tube provided with the flasks was attached to the end of the hose coming from the well, and was purged for several minutes. The fill tube was then attached to the flask, and water was allowed to fill the flask until approximately 700 cm^3 of water was in the flask. Flasks were then shipped to Isotech Laboratories for analysis of methane concentration, gas isotopes, and gas composition.

Gas composition for all sampling techniques was measured using a gas chromatograph. Gas isotopes were measured by gas combustion and isotope ratio mass spectrometry (IRMS). Methane concentration was measured using a headspace equilibration technique developed by Isotech Laboratories, Inc. For some samples, hydrogen isotopes of methane were measured using Cavity Ring-

Table 2
Dissolved organic carbon (DOC) and acetate concentrations measured in water samples from the wells at the Birney test site. Acetate concentrations <1 mg L^{-1} are below the level of reliable detection and reported values are semi-quantitative. nd = no data (Sample not collected).

Coal bed	Date	DOC (mg L^{-1})	Acetate (mg L^{-1})
Knobloch	5/15/2013	3.51	0.3
	8/01/2014	3.69	nd
Nance	5/15/2013	3.08	0.1
	8/01/2014	2.4	nd
Flowers-Goodale	5/14/2013	3.05	0.5
	9/25/2013	2.93	0.6
	8/01/2014	2.67	nd
Terret	5/14/2013	1.75	0.2
	8/01/2014	nd	nd

Down Spectroscopy (CRDS). Detailed analysis information is available through Isotech Laboratories, Inc. (www.isotechlabs.com).

2.4. Hydrologic testing

2.4.1. September 2013 aquifer test

The production well for this test (FGP-13) was instrumented by installing a Bennett™ pump at a depth of about 112.8 m. Water levels were recorded in the production well (FGP-13) and in observation wells FG09, FG-11, FGM-13, SS-13, N-11, and T-09 using In Situ™ Level Troll unvented transducers. Pumpage was started at 16:30 on September 23 and ended at 12:00 on September 25. Observations of water-level recovery continued until 14:20 on September 27. Initial depths to water for all monitored wells are listed in Table S2. Well discharge was determined from 16 volume-discharge measurements (time to fill calibrated vessel), ranging from 0.95 to 2.46 liters per minute (Lpm), with a time-weighted mean of about 1.32 Lpm.

2.4.2. July 2014 aquifer test

Determination of the anisotropic transmissivity tensor requires data from three observation wells, all oriented at different directions from the production well. This requirement wasn't met for the September 2013 test because of the failure of well FGM-13 to provide data analyzable using a porous-media model. Consequently, a second test was conducted in July 2014 by pumping well FG-11 and monitoring drawdowns in wells FG-09, FGP-13, FGM-13, and SS-13. (Because no drawdowns were detected in the Nance or Terret wells during the September 2013 test, these wells were not instrumented for the July 2014 test.) This test was instrumented on July 21, 2014. In Situ™ Level Troll 300 unvented transducers were installed in the pumped well and in the four observation wells and the Bennett™ pump was installed in well FG-11 at a depth of about 107 m. The aquifer test was begun at 09:41 on July 22, with pumpage continuing until 11:31 on July 24. Water level recovery was monitored until about 11:30 on July 26. Discharge records for the test included 13 volume-discharge measurements, which provide well discharges ranging from 1.85 to 3.40 liters per minute (Lpm) and averaging about 2.65 Lpm. Specific capacity (discharge per m of drawdown) was about 0.093 Lpm per meter of drawdown (Lpm/m), compared to the specific capacity for well FGP-13 of 0.018 Lpm/m (Table S3).

2.4.3. Aquifer-test analysis

Analysis of the aquifer tests requires that a number of assumptions be made concerning the aquifer, the underlying and overlying formations, and the well. The main assumptions regarding the aquifer include: uniform thickness, uniform hydraulic properties (transmissivity and storage) in time and space, and substantial areal extent of the aquifer. The underlying and overlying formations are assumed to be spatially uniform in their properties, and to be much less permeable than the aquifer. For the aquifer test analysis, the aquifer is also assumed to rest on an impermeable base, to be anisotropic and to exhibit dual porosity, and to be overlain by a semi-confining bed in turn overlain by a constant-head source bed. Well bore storage and production well skin effects are assumed. The Flowers-Goodale wells are assumed to be fully penetrating, despite the fact that they are equipped with 3 m screens, except for FGM-13, which has a 1.5 m screen. All screen lengths are less than the 5.5–7.3 m thickness of the Flowers-Goodale, but the wells are sand-packed over most or all of the full thickness of the coal (Table S1). For such a low permeability aquifer and low pumpage rates, head losses through the sand pack are likely quite small, so the wells are assumed to fully penetrate the aquifer.

2.4.4. The mathematical models

Aquifer-test analysis requires the selection of a solution that adequately provides an idealized representation of the hydrologic regime prevailing at the test site. When aquifer anisotropy is anticipated, two sets of analyses are required, one assuming isotropy, in which the solved-for transmissivity value is that equal to the effective T, $T_e = \sqrt{T_{xx}T_{yy} - T_{xy}^2}$ or $\sqrt{T_{\xi\xi}T_{\eta\eta}}$, where $T_{\xi\xi}$ is transmissivity in the direction of maximum T and $T_{\eta\eta}$ the transmissivity in the minimum direction (Weeks, 2005). Drawdown data for each of the three needed observation well locations are analyzed as though they are derived from an isotropic aquifer, and the results then analyzed for the anisotropy tensor.

For the initial isotropic analyses, the Flowers-Goodale tests were analyzed using the Case 3 solution (Moench, 1985, 1984), as implemented for the Aqtesolv™ software package (Duffield, 2007). This program provides a means of evaluating tests either of leaky aquifers or of confined dual-porosity isotropic aquifers, and includes means of accounting for effects of wellbore storage and well skin. Use of this model to analyze the Flowers-Goodale test data requires additional assumptions, because the aquifer is assumed to be both a dual-porosity and a leaky aquifer. For our analyses, a single semi-confining bed overlain by a constant-head source bed was assumed. In this application, the term effective radius of the borehole (r)/thickness (B′), where $B' = \sqrt{\frac{Tb'}{K_v'}}$, is treated as a fitting factor that mimics the combined effects of matrix-fracture fluid transfer and leakage from the upper and lower semiconfining beds combined; and $B' = (\frac{r}{4B'}\sqrt{\frac{b'S_s'}{S_f}})$,(where S′ = the storage coefficient of matrix and S_f = storage coefficient of fractures) the combined storage effects of the coal matrix and the two semi-confining beds.

Methods and equations for performing the transmissivity anisotropy analysis have been previously described (Papadopulos, 1965; Weeks, 2005).

2.5. Microbiological methods

2.5.1. Cultivation experiments

Twenty core samples were collected at different depths throughout the Flowers-Goodale coal seam and adjacent sand- and silt-stones in order to characterize microbial capabilities to utilize electron acceptors (nitrate, sulfate, oxygen). To create an inoculum, a 20 mL volume of each coal sample (measured by displacement) was crushed and added to 60 mL of dilution medium [2.5 g/L NaHCO3, 0.1 g/L KCl, and a surfactant, Tween 80 (0.02%) prepared under N_2/CO_2 (80:20)], in a N_2 filled glove bag in the field. Media was designed for selective enrichment of metabolic characteristics of interest (i.e. sulfate reduction). All anaerobic media were defined, inorganic bicarbonate buffered media with added electron acceptors and electron reducers to define metabolic capabilities (Jones et al., 2008). Nitrate medium had 10 mM acetate and 8 mM nitrate added and SO_4 medium had 10 mM each SO_4 and lactate and was further reduced with L-cysteine HCl. Formation water samples from the Flowers-Goodale, Terret, and Knobloch coal seams were also tested for microbial capabilities. In order to compare formation water samples with coal samples, the sample volume was adjusted (from 30 mL to 1 mL) to account for the small volume of water present in coal. All samples were returned to the lab the following day, and the headspace was replaced with N_2:CO_2 (80:20). Each sample bottle was placed in a sonifying bath for 5 min. A 0.5-mL volume of the liquid was transferred under sterile conditions using a needle and syringe into triplicate 28-mL Hungate tubes containing 10 mL of each dilution medium and fitted with Teflon coated stoppers (West Co.). The tubes were incubated statically, in the dark, at 22 °C for 10 months. To determine if sulfide was produced in sulfate media, a drop of sample was applied to a lead acetate strip after 6 weeks culture incubation. Samples in nitrate media were checked for cell growth after 10 days incubation. Media with potential organic substrates were sampled for methane after at least 100 days by removing 0.3 mL of the headspace through the stopper using a gas-tight syringe equipped with a locking valve and analyzing by gas chromatography (GC) using the methods described in Jones et al. (2008).

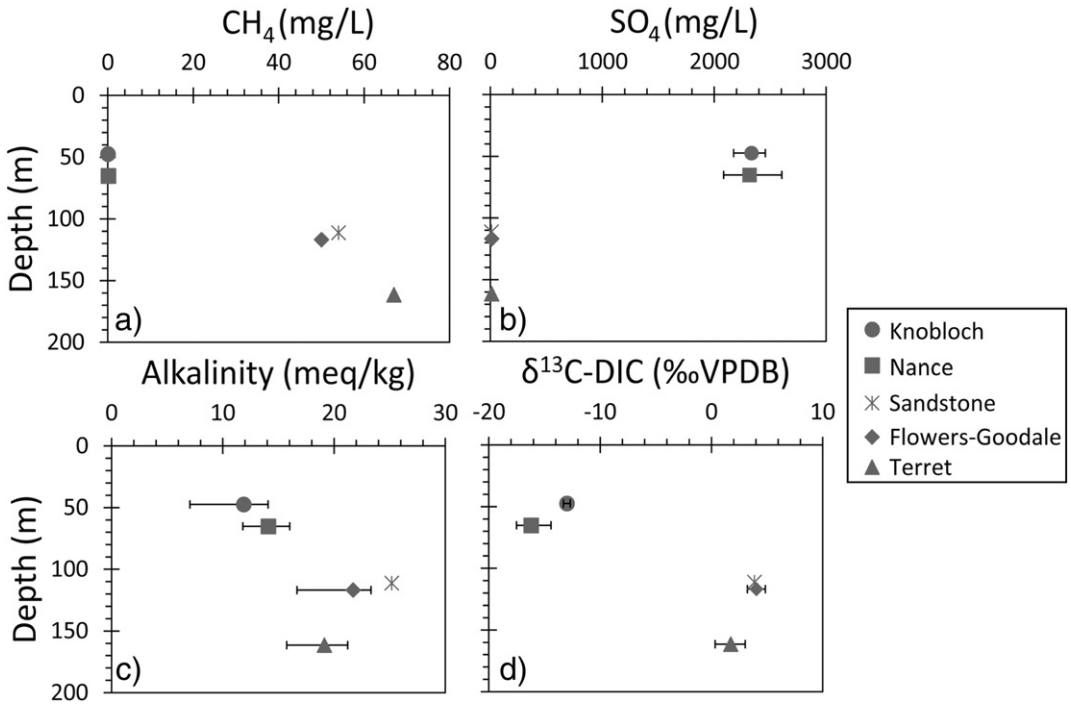

Fig. 3. Dissolved methane (a), sulfate (b), and alkalinity (c) concentration, together with the $\delta^{13}C$ value of dissolved inorganic carbon [DIC (d)] in groundwater from individual coal seams and adjacent sandstone. Where multiple samples from the same well were collected, the mean concentration is shown and bars represent the range of values measured.

2.5.2. Bioassays

The Flowers-Goodale core (FG-11) was sampled to examine differences in bioavailabilty of organics across the boundaries and through the coal seam. Sections of fresh core were transferred into a glove bag purged with N_2, sectioned into fine depth intervals, and transferred into glass jars with air tight seals. Twelve samples of coal, 4 of overlying sand, 2 in a siltstone parting, and 3 in the siltstone at the base of the coal seam were collected. These samples were kept cool (4 °C) and returned to the lab for processing. The jars were opened in a Coy Anaerobic chamber filled with $N_2/CO_2/H_2$ 85:5:10. Coal samples (and adjacent intervals composed of sand or silt) were broken up into chunks that could pass through the opening of a serum bottle (1 cm diameter) and 7 g were loaded into each 120-mL serum bottle. Anaerobic fresh water medium (60 mL) was added and the bottles were sealed, as previously described (Jones et al., 2008). The medium was composed of (per liter ultrapure water) 2.5 g $NaHCO_3$, 0.5 g NH_4Cl, 0.5 g NaH_2PO_4, 0.1 g KCl, and trace minerals and vitamins (Jones et al., 2010). After bottles were removed from the anaerobic chamber, the headspace was replaced with N_2/CO_2 (80:20) to remove H_2 and maintain correct pH buffering. Bioassays were performed as previously described (Jones et al., 2008). There were 4 treatments, each conducted in duplicate for each sample. Two treatments included the addition of mixed cultures in order to assay bioavailable organics in the coal: WBC-2 (as described in Jones et al., 2008) and WBC-4 (similar culture maintained on soybean oil and optimized for degradation of coal-methane intermediates). WBC-2 generally produced methane more rapidly than WBC-4, but both cultures were similar in terms of the total amount of methane produced, and only results from WBC-2 are shown. In a third treatment, no culture was added, in order to assess methane production by the native microbial population. In a control treatment, bromo ethane sulfonate (BES), an inhibitor of biomethanogenesis, was added to account for methane desorbed from the coal during incubation. Methane was also monitored in treatments without coal to ensure the cultures were not producing methane in the absence of coal. An initial measurement of headspace methane was made, and bottles were then incubated in the dark at 22 °C. The headspace was monitored weekly for changes in methane content for 6 weeks. The amount of methane released in each sample treated with BES (*i.e.* the amount of desorbed methane) was subtracted from the amount of methane in treatments where biomethanogenesis was not inhibited in order to determine the amount of methane attributable to added cultures or native microbial communities.

2.5.3. Pyrosequencing analysis

Pyrosequencing was used to characterize the microbial populations from the cores. DNA was extracted from the inner portion of the core samples by using a sterilized chisel to remove the outer 1–2 cm of core and the bacterial and archaeal small subunit (SSU) rRNA genes were amplified as previously described (Barnhart et al., 2013). The bacterial primers included: barcoded FD1 (5′-AGAGTTTGATCCTGGCTCAG-3′) and non-barcoded 1540R (5′-GGAGGTGWTCCARCCGC-3′) in the initial amplification and barcoded FD1 and barcoded 529R (5′-GGCA GATTCTTTGCCTTCTG-3′) in the second round of amplification (Bowen De León et al., 2013; Yakimov et al., 2001). The archaeal primers included: 21F (5′-TTCYGGTTGATCCYGCCRGA-3′) and 1492R (5′-CGGT TACCTTGTTACGACTT-3′) and barcoded 751F (5-′ CCGACGGTGAGRGRYGAA-3′) and 1204R (5-TTMGGGGCATRCIKACCT-3′) (Baker et al., 2003). A 0.8% agarose gel in Tris-Acetate-EDTA buffer was used to check the PCR products for DNA of the correct size. Archaeal SSU rRNA genes were not amplified, suggesting the archaea in the core materials were below detection limits. The gel extracts from the bacterial SSU rRNA amplicons were cleaned and concentrated using the Wizard SV Gel and PCR Cleanup System® (Promega, Madison, WI), and dsDNA was quantified with a Qubit fluorometer (Life Technologies, Carlsbad, CA, USA). Adaptors for 454-pyrotag analysis were ligated to the amplicons and were pyrosequenced in a Roche 454 GS-Junior (454 Life Sciences, Branford, CT, USA). The barcoded sequencing reads were separated by Roche's image analysis and sequence assignment software providing high confidence in assigning sequencing reads to the appropriate sample.

Pyrosequences were trimmed to one standard deviation below the mean (removed if shorter), subjected to varying quality (Q) cutoffs (25, 27, 30, and 32) allowing either 10% or 15% of the nucleotides to

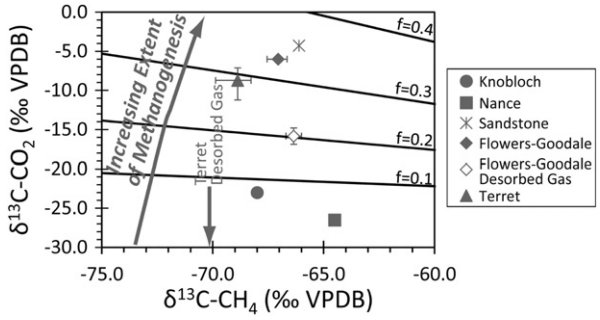

Fig. 4. Stable carbon isotope composition of dissolved methane and carbon dioxide in groundwater from individual coal seams and adjacent sandstone. Where multiple samples from the same well were collected, the mean concentration is shown and bars represent the range of values measured. Desorbed gas samples from the Flowers-Goodale and Terret (δ^{13}C-CH_4 only; there was not enough CO_2 to measure isotopic composition) coals are also shown for reference. The black lines with *f* values represent the fraction of available organic (coal) carbon that has been converted to methane based on the δ^{13}C values of CO_2 and CH_4. A higher *f* value represents a greater extent of methanogenesis compared to other terminal electron accepting processes, such as sulfate reduction.

be below the cutoff, and removed if primer errors or ambiguous nucleotides were observed as previously described (Bowen De León et al., 2012). Forward reads were carried through the analysis. A python script was used for data management and analysis as previously described (Bowen De León et al., 2012). Chimeras were removed using ChimeraSlayer (Haas et al., 2011). The ribosomal database project (https://rdp.cme.msu.edu/) RDPipline was used to select operational taxonomic units (OTUs) and the statistical package R was used to standardize and group the OTUs (Yoder, 2013).The bacterial communities were diverse and only OTUs composing >1% of the community were represented with a heat map. Linear discriminant analysis and effect size statistical methods (LEfSe) were used to identify bacterial species correlated with coal and non-coal samples (Segata et al., 2011).

3. Results and discussion

3.1. Core and coal characteristics

Desorbed gas was only detected in samples obtained from the Flowers-Goodale and Terret coal beds (Table 1). Total gas content (TGC) concentrations ranged from 16.64 to 19.21 standard cubic feet per ton (scf/ton) in the Flowers Goodale and 11.21 scf/ton in the Terret. Ultimate and proximate analysis indicates the coals are subbituminous C in rank, have low sulfur contents that are dominated by organic sulfur, and have relatively low ash yields. (Table S4).

3.2. Chemistry of formation water and gas

DOC values for all coal beds at the site ranged from 1.75 to 3.69 mg L^{-1} (Table 2). A sample for DOC was not collected from the Terret on 8/1/2013. These are within the range of values for DOC observed in produced water or formation water from similar coal beds (Orem et al., 2014). The Knobloch (shallowest coal) had the highest DOC values, and the Terret (deepest coal) had the lowest, however, this observation is based on very limited sampling. Repeat sampling of the Knobloch, Nance, and Flowers-Goodale coal beds from 2013 and 2014 exhibit similar concentrations, suggesting relative steady state in DOC concentrations (Table 2).

Only acetate was observed in the VFA analysis, and was just above detectable levels in the formation waters for all of the coal beds (Table 2). All acetate concentrations were below 1 mg L^{-1}. The presence of VFAs in formation water reflects a balance between bacterial biodegradation of higher molecular weight organic substances to produce VFAs (especially acetate), and consumption of VFAs by terminal microbes in the biodegradation pathway, such as sulfate-reducing bacteria and methanogenic archaea.

Relatively high methane concentrations (50 to 67 mg L^{-1}) were measured in the two deepest coal beds sampled (Flowers-Goodale and Terret) and an adjacent sandstone well (Fig. 3a). In contrast, there was very little (0.02 to 0.015 mg L^{-1}) dissolved methane detected in the two shallowest coal seams (Knobloch and Nance). These results are consistent with the TGC measurements from the coal cores, where the highest TGC was observed in the Flowers-Goodale and Terret coals (Table 1) although the core samples from the Flowers-Goodale had slightly higher TGC concentrations. Desorbed gas was not detected in the Nance or Knobloch coals. Sulfate concentrations in coal formation waters display the opposite trend of methane with depth (Fig 3b). The highest sulfate concentrations (20–25 mmol L^{-1}; average value of repeat samples; raw data shown in Table S5) were measured in the shallowest coal seams (Knobloch and Nance), while sulfate was not detected in the deeper coal seams (Flowers-Goodale and Terret) or the adjacent sandstone. Nitrate was below detection in all coal bed water samples.

The δ^{13}C values of the dissolved methane ranged from −70‰ to −64‰ (Fig. 4). These highly negative values clearly indicate a microbial origin for the natural gas (Whiticar et al., 1986; Whiticar, 1999), and are within the range of commercial CBM wells in the area (Bates et al., 2011; Flores et al., 2008). Furthermore, the low abundance of ethane (<0.02 mol%) and lack of detectable higher chain hydrocarbons (Table S5) further confirm the absence of significant thermogenic gas and dominance of biogenic methane. Alkalinity concentrations, which are equivalent to dissolved inorganic carbon (DIC) concentrations in these waters (Bates et al., 2011), increased with depth from 12 to 22 meq/kg (Fig. 3c). δ^{13}C values of DIC in groundwater also increased from and −16 to +4‰ with depth (Fig. 3d). High alkalinity concentrations, typically >15 meq/kg, and especially relatively high δ^{13}C-DIC values (>0‰), indicate microbial methanogenesis (McIntosh and Martini, 2008). Bacterial sulfate reduction also can produce alkalinity concentrations >10 meq/kg. However, the δ^{13}C-DIC value after sulfate reduction is likely to be consistent with the isotopic composition of the source organic carbon (coal) (Clark and Fritz, 1997). The δ^{13}C values of PRB coal is approximately −25‰ (Formolo et al., 2008; Holmes et al., 1991). The δ^{13}C values of CO_2 are essentially bimodal, with the most negative values in the Knobloch or Nance (−26.5‰ to −22.4‰) and higher values in the Flowers-Goodale, sandstone above Flowers-Goodale, and Terret (−11.2‰ to −4.3‰; Table S5). Variations in δ^{13}C-CO_2 correspond with the large decline in sulfate concentration with depth below the Nance coal (Fig. 3b).

A mass balance calculation between methane and CO_2 produced from coal-derived organics can be used to define the extent of methanogenesis relative to other pathways, such as sulfate reduction, that compete for organic substrates but do not produce methane. This balance is represented by $\delta^{13}C_{org} = \delta^{13}C\text{-}CH_4 \times f + \delta^{13}CCH_4 \times (1 - f)$, in which $\delta^{13}C_{org}$ is the δ^{13}C of bioavailable substrates that bacteria and archaea can consume (Blair, 1998). Here again, the bimodal character of the coal bed water chemistry is seen in estimated values of *f*, the extent of methanogenesis relative to other pathways. In the Knobloch and Nance coals, the more negative δ^{13}C-CO_2 values, together with consistently low δ^{13}C-CH_4 values, correspond to low extents of methanogenesis ($f < 0.1$) in which relatively little of the available coal organic carbon is converted into methane, likely instead being consumed by sulfate reduction or other bacterial processes (Fig. 4).

The largest extent of methanogenesis at this site ($f > 0.3$) was observed in the Terret and Flowers-Goodale coals, with the Flowers-Goodale coal having a slightly greater extent of methanogenesis than the Terret coal (Fig. 4). This is consistent with their high dissolved methane concentrations, TGC, and groundwater geochemistry indicative of microbial methanogenesis. Together, the water and gas geochemistry data show that the deepest coal seams, the Flowers-Goodale and Terret,

and adjacent sandstone are within the methanogenic zone, whereas the shallowest coal seams (Knobloch and Nance) are predominantly sulfate-reducing. The high sulfate concentrations in groundwater appear to be the major inhibitor of methanogenesis in the shallowest coal seams. Consistent with other studies and environments, millimolar concentrations of sulfate (>100 mg L^{-1}) permit sulfate-reducing bacteria to consume organic substrates, largely outcompeting methanogens for these carbon sources and preventing methanogenesis (Capone and Kiene, 1988; Whiticar et al., 1986).

3.3. Hydrology and hydrologic testing of Flowers-Goodale coal bed

3.3.1. The September 2013 aquifer test

The pumpage-induced drawdowns observed in the three observation wells tapping the Flowers-Goodale and the well tapping the overlying sandstone are shown in Figure 5. For an ideal isotropic aquifer, the composite log-log plot of drawdowns for the three Flowers-Goodale wells would show three closely overlapping curves, and for an ideal anisotropic aquifer (such as expected for coal aquifers), the composite log-log plot of drawdowns for the three Flowers-Goodale wells would show three curves for which early time drawdowns were separated from each other by a constant amount in log space. As shown in Fig. 5, this anisotropic condition is approximately met by drawdown data for wells FG-09 and FG-11, with larger drawdowns throughout for well FG-09 relative to those for well FG-11. The much greater relative flattening of drawdowns in well FG-11 at later times relative to those for FG-09 is suggestive of greater leakage in the vicinity of well FG-11, as will be discussed later. However, drawdowns in FGM13 and SS-13 show patterns that are completely inconsistent with those expected for porous (or dual-porosity) media, as drawdowns in the two wells start immediately and increase linearly in log-log space, resulting in drawdown curves that cross those for wells FG-09 and FG11. The FGM-13 and SS-13 plots approximate an early-time log-log half slope. Such behavior is suggestive of the presence of a dominant fracture passing through the production well and through or near to the affected observation wells.

3.3.2. The July 2014 aquifer test

Drawdown data for all four observation wells obtained during the July 2014 test are shown as a composite plot in Fig. 6. Comparison with Fig. 5 indicates that, for the 2014 test, drawdowns in wells FGM-13 and SS13 show early time behavior that, unlike for the 2013 test, is consistent with that expected for a porous media aquifer. Early data for well FGM-13 superimpose closely on the data for FGP-13, as would be expected. However, FGM-13 drawdowns level off dramatically relative to those for well FGP-13 after about 100 min. The drawdown behavior for well FGM-13 thus remains anomalous. Drawdown response in the sandstone well, which taps a different aquifer, now lags, on a t/r^2 (time divided by distance between pumped, observation wells) basis.

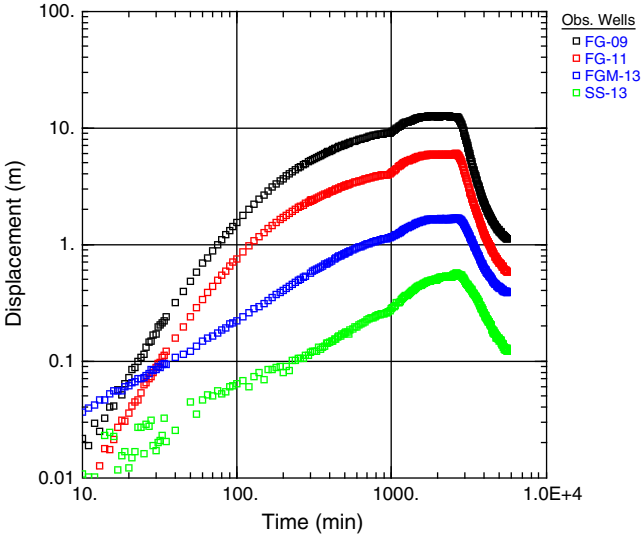

Fig. 5. Composite log-log plot of drawdowns for the four affected observation wells, as observed during the September 2013 Flowers-Goodale aquifer test.

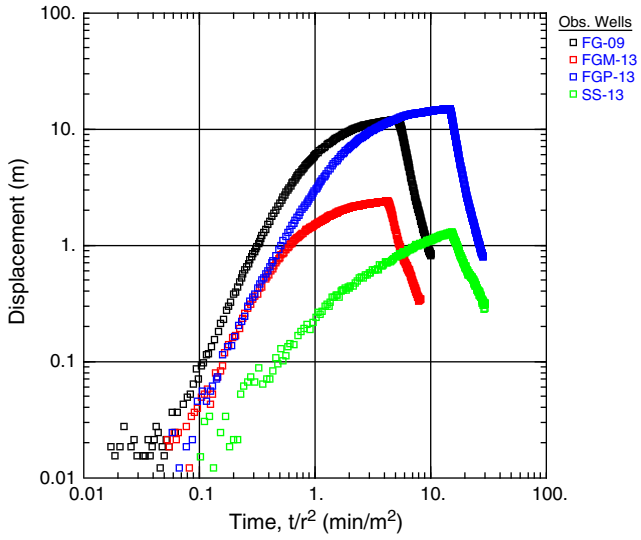

Fig. 6. Composite log-log plot of observation well drawdown data for the July 2014 test. The time axis has been converted to t/r^2 to account for the delay in timing with distance from the production well.

The composite drawdown plots for wells FG-09 and FGP-13 (Fig. 6) are parallel in log-log space until drawdowns in each well reach about 3 m, after which drawdowns in both wells begin to flatten, presumably due to leakage from the overlying sandstone, but with more rapid flattening in the more distant well FG-09. Thus, the combined results from the two aquifer tests should provide adequate data to analyze for the transmissivity vector, based on FGP-13—FG-09, FG11—FG-09, and either FGP-13—FG-11 or FG-11—FGP-13 data.

3.3.3. The test analyses

Numerous isotropic leaky-aquifer test analyses were made using drawdown data collected from the pumped wells themselves and from the pumped well-observation well pairs FGP-13-FG-09, FGP13FG11, FG-11-FGP-13 and FG-11-FG-09. Although these analyses indicated that ranges of parameters provide equally adequate curve matches, their combined results help to provide confidence in certain parameter values. As an example, the bulk of the analyses indicate that the effective transmissivity (T_e) value should be in the range 0.02–0.05 m^2/d, with the mid-point value 0.0325 m^2/d being a best estimate (Weeks, 2005). For the final analyses, T_e was set to the mid-point value, with adjustments for other parameters made to achieve a fit. The analyses also indicated that Ws (well skin) values could be varied substantially, with changes in Ws resulting in adjustments for T, r/B′, S, and β′. However, the ranges of fitted well skin results varied between the evaluation of pumped well data, which required negative skin values to obtain an optimum fit, and observation well data that could be matched using various values of skin if other hydraulic properties were allowed to vary. The skin value should instead be constant for all analyses for a given pumped well. The most consistent estimate of skin is that it is about 0, and that value was fixed for the final analyses.

Results of the final analyses for well pair FGP-13—FG-11 (Fig. S2), well pair FG-11—FGP-13 (Fig. S3), well pair FGP-13—FG-09 (Fig. S4), and well pair FG-11—FG-09 (Fig. S5) are listed in Table S6. These

analyses provide T_e of 0.0325 m^2/d, and S_c values ranging from 1.2×10^{-5} to 1.6×10^{-5}. The semi-confining bed properties, tabulated as dimensional B (m) values ranging from 24 to 66 m, and β/r (m^{-1}), ranging from 0.0057 to 0.037/m, show large variance, as might be expected for such an ill-defined layer. Differences between the solved for B and β values for the two well pairs FGP-13 and FG11 should be identical, and they are not.

The x-y coordinates for the observation wells relative to the pumped well are needed for the anisotropy analysis. Distances and bearings to the observation wells from the pumped well (FGP-13 or FG-11) were obtained using the Path Tool in Google Earth. Bearings were converted to angles from due east measured counter-clockwise, thus assuming that the x axis is oriented east-west. The x-y coordinates were then computed based on trigonometric considerations, as shown in Table S7. Computation of the transmissivity anisotropy also requires evaluation of $4T_e^2t_1$, where $t_1 = r^2S_c/4T_e$, or $T_eS_cr^2$ from the specified r values for each well and the T_e and S_c values provided in Table S6.

Two sets of anisotropy analysis were made, based on head values listed in Table S2. For the first set, data for the well pairs FGP13FG09, FGP-13-FG-11, and FG-11-FG-09 were used to develop one equation set. For the second set, the well pairs used were FGP-13–FG-09, FG11–FGP-13, and FG11–FG09. These data were analyzed for the various anisotropy variables using an xcel™ spreadsheet. The resulting $T_{\xi\xi}/T_{\eta\eta}$ ratios of 1.47 and 1.35 (Table 3) are plausible. Differences in the ratio due to the difference in parameters determined from the FGP13–FG-11 and FG11–FGP13 pairs is small, but the difference in bearing of the major transmissivity axis is significant, varying by about 35°.

Hydraulic heads, head gradients, and local flow direction.

Completion of wells in different coal beds at the Birney test site led to the surprising finding that the hydraulic head, as indicated by depths to water, in the different coals varied substantially. The greatest depth to water (lowest hydraulic head) occurs in the intermediate depth Flowers-Goodale. The relatively steep vertical hydraulic gradients, downward from the Knobloch and upward from the Terret, toward the Flowers-Goodale suggest that the Flowers-Goodale acts as a groundwater drain to the Tongue River, located about a mile away at its nearest point. The downward flow in coal seams above Flowers-Goodale to the Flowers-Goodale fits with the transition in redox gradients. The Flowers-Goodale also has the greatest extent of methanogenesis, suggesting that longer residence times may be a key factor in the amount of the carbon pool that has been utilized by the bacteria and methanogens.

The magnitudes and directions of the hydraulic head gradients were evaluated using relative altitudes of the well measuring points, obtained with a precision of 0.0003 m with a Trimble DiNi digital level, along with depth to water measurements to the same precision. These data allow the computation of hydraulic heads for each well (Table S2).

The magnitude and bearing of head gradients in the Flowers-Goodale were evaluated using the three-point method. Briefly, the three-point method relies on the use of head data from three wells, the locations of which form the vertices of a triangle. These vertices represent high head (H_H), low head (H_L), and intermediate head (H_I). The strike of the head gradient is determined by interpolating the point H_{int} on the H_HH_L line that is equal to H_I. The bearing of the line connecting H_I to H_{int} provides the strike, and H_L-H_{LI}, the down-gradient perpendicular to that line, the head gradient bearing. The down-gradient distance from the strike line to H_L is given by (H_IH_L) sin(θ), where θ is the angle separating the H_I-H_L and H_I-H_{int} lines.

The magnitude and bearing of head gradients in the Flowers-Goodale were computed using head data collected for wells FG-09 (H_I), FG11 (H_H), and FGM-13 (H_L) on November 17, 2014 (Table S2). The solution of the three-point method indicates that the bearing of the strike line is N25°E, the steepest gradient is at N65°W, and the head gradient is 0.00317 m/m or 3.17 m/km. Computations were also made using the water level depths measured at the start of the July 2014 aquifer test (Table S2). Water levels for all the Flowers-Goodale wells were about 0.3 m higher than in November, and showed FG-11 as the intermediate-head well, with FG-09 being the high-head well. The strike line for these data provides a bearing of N35°E, so the gradient direction is N55°W, 10° more northerly than that determined for the November data. The gradient for these head data is 0.00307 m/m or 3.07 m/km, very similar to that for the November data.

3.3.4. Effects of transmissivity anisotropy

Transmissivity anisotropy results in the groundwater flow direction deviating from that of the steepest head gradient unless the head gradient is aligned with the major transmissivity axis. The bearing of the flow direction in an anisotropic aquifer may be found using the equation (Maasland, 1957) $\alpha = \arctan[(T_{\eta\eta}/T_{\xi\xi}) / \tan(\phi)]$, where α is the angle measured counterclockwise from the principal transmissivity axis, and ϕ is the angle formed by the intersection of the head gradient strike with that axis. Based on the July 2014 head gradient analysis and the FG-11—FGP-13 anisotropy analysis (Table 3), $\alpha = \arctan[(0.028/0.038) / \tan(\phi)]$, where ϕ is the angle between the transmissivity vector (N18.1°W) and the head gradient strike (N35°E), or 53.1°. Flow direction is found by the counter clock-wise addition of the resulting α of 28.8° to the transmissivity axis bearing to obtain the flow direction bearing of N47°W, compared with the uncorrected bearing of N55°W. Based on the November 2014 head gradient analysis and the FGP-13—FG-11 anisotropy analysis (Table 3), $\alpha = \arctan[(0.027/0.039) / \tan(89.5°)]$ or 0.006°. Thus, the bearing computed from these data is nearly identical to the uncorrected flow direction. This correction is small because the head gradient is almost exactly aligned with the major transmissivity axis.

Results of the gradient and bearing calculations are plausible, but represent values over a small local area. Their relevance to the regional Flowers-Goodale head gradient and its bearing may be evaluated by extrapolation of the flow direction bearing to the Tongue River. Extrapolation of the flow direction of N47°W, determined from the July head data, leads to the Tongue River at its nearest point (about 1707 m), which fits with the logic that the river is the discharge point for the shallower aquifers at the Birney test site. However, based on the Google Earth land surface altitude for the site of 962 m and an assumed height of the well measuring points above land surface of 0.61 m, head altitude of the Flowers-Goodale well cluster is about 925 m. The Google-Earth river altitude at its nearest point is 922 m, only 2.4 m lower than the well-cluster head. The river is about 1707 m removed, and a gradient of 0.0031 m/m indicates a head drop of 5.18 m, which is below river level. The steep gradient to the NW may manifest local conditions, including the effect of the very low transmissivity of the Flowers-Goodale at the site. The regional Flowers-Goodale head gradient is likely

Table 3
Results of the Flowers-Goodale anisotropy analyses, as computed using an excel spreadsheet. The large number of decimals retained are to facilitate comparison between the two solutions, and should not be construed to imply accuracy.

STxx	STyy	STxy	S ($X10^{-5}$)	Tξξ	Tηη	Ratio	Bearing of Tξξ,	Remarks
M^4/d ($X10^{-8}$)				m^2/d				
3.797	3.355	−0.6383	1.16	0.039	0.027	1.47	N54.45°W	FGP-13—FG-11
3.707	4.735	0.3749	1.38	0.038	0.028	1.35	N18.1°W	FG-11—FGP-13

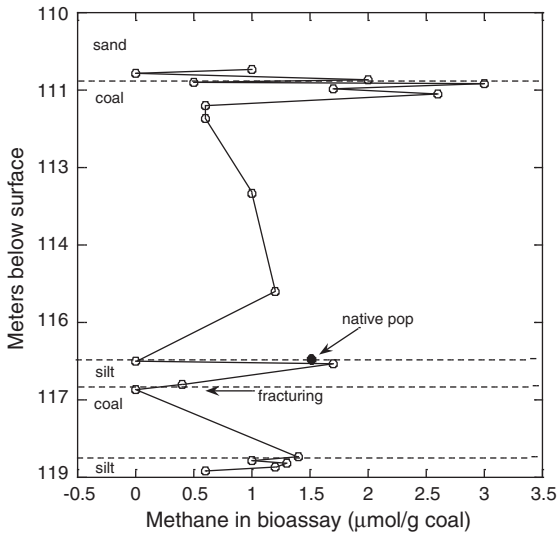

Fig. 7. Bioassay results indicate the coal is most bioavailable to WBC-2 at the upper interface of the Flowers-Goodale coal bed. Methane production was monitored from 19 coal samples and only one sample produced methane from the native population that was obtained near a bottom interface of the coal seam.

much shallower, and oriented toward the NE, sub-parallel to but still reaching the Tongue River at a point downstream.

3.3.5. Vertical head gradients

Head gradients vary substantially with depth, downward above the Flowers-Goodale and upward from deeper beds. For example, hydraulic heads of the Knobloch of 932 m and of the Nance of 926 m, separated by about 12 m of siltstone, imply a downward vertical head gradient of about 0.5 m/m. Surprisingly, the vertical head gradient between the Nance and the screened interval of the sandstone well is only about 0.03 m/m, despite the presence of about 12 m of siltstone and 3 m of mudstone separating the units. Head in the sandstone well is slightly higher (0.07–0.15 m) than in the nearby Flowers-Goodale wells, providing a vertical downward gradient of about 0.01–0.02 m/m. Heads in the Flowers-Goodale of 925 m, and in the Terret well T-09 of 940 m imply an upward vertical head gradient of about 50 m/130 m or 0.4 m/m. The large difference in heads between the T-09 and T-11 wells of 1.6 to 1.3 m is unexplained. The steep upward gradient between the Flowers-Goodale and Terret coals indicate that one or more of the three siltstones occurring between the coal beds represent a tight confining layer.

The coal bed hydraulic properties are estimated to be lower than observed for other PRB coal beds. The comparisons are best made by adjusting for differences in test-site aquifer thickness by computing K_e (hydraulic conductivity $= T_e/b$) and S_s (specific storage $= S/b$). The Flowers-Goodale K_e for this site is about 0.005 m/d, and S_s about 2×10^{-6}/m. For example, the K_e for this site is about 200 times smaller than the value of 1.2 m/d determined for the Flowers-Goodale coal at the NC02–2 site, located about 9.6 km to the west southwest (Weeks, 2005). Further comparison is provided by the compilation of 172 hydraulic conductivity values determined for coals in northeast Wyoming, southeast Montana, and western North Dakota (Rehm et al., 1980). That compilation provides a geometric mean K_e value for the various coals of about 0.46m/d, nearly 100 times greater than our calculated Flowers-Goodale value. Statistical analyses of the compiled results by Rehm et al. (1980) indicate a $\log_{10}\sigma$ (standard deviation) of K_e for the coal beds of about 1. Thus, K_e for the Flowers-Goodale at our site is about 2σ smaller than the geometric mean. The low K_e value determined here appears to be anomalous. However, despite problems of non-uniqueness and of likely large spatial variability of semi-confining bed properties, the K_e value determined here is probably correct within a factor of 2.

The S_s value of about 2×10^{-6}/m for the Flowers-Goodale at the Birney site is also anomalously low, being an order of magnitude smaller than that of 2×10^{-5}/m determined for the same coal at the NC02–2

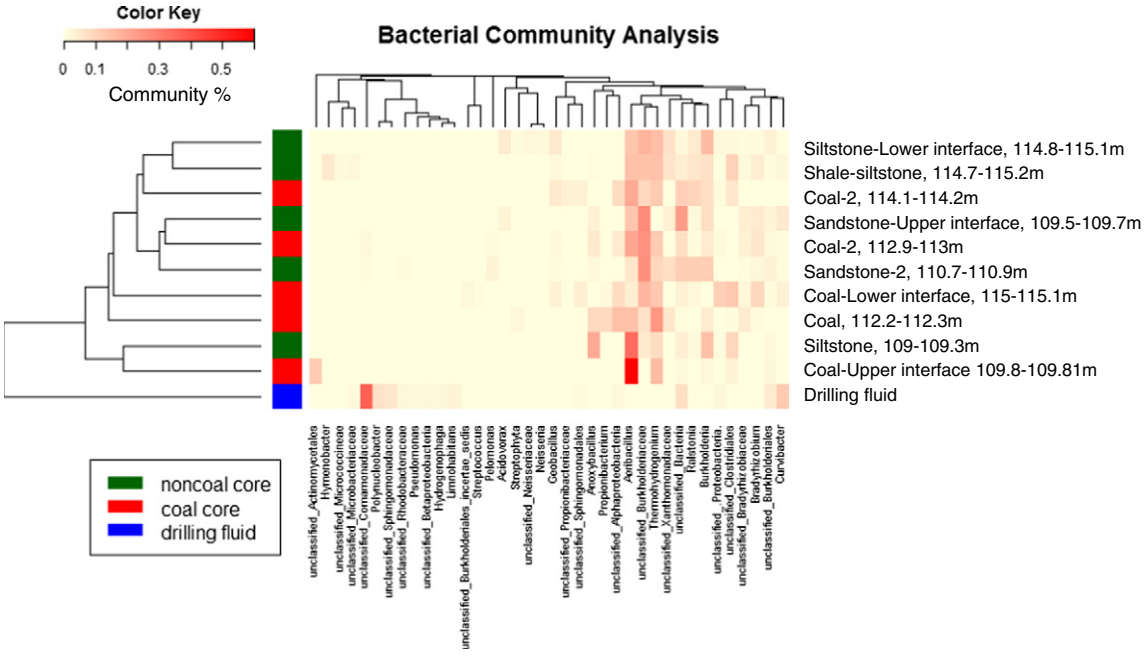

Fig. 8. Heatmap representing 454-pyrotag sequencing analysis of the 16S-rRNA gene of the bacterial community from two separate core samples of the Flowers-Goodale coal and one drilling fluid sample. The samples were grouped with Bray Curtis statistics. The bacterial operational taxonomic units (OTUs) that composed >1% of the microbial community are listed at the bottom of the heatmap. The samples that were analyzed are listed on the right of the heatmap and core samples from T-11 coring are denoted with −2 (see Fig. S1 for exact locations).

site (Weeks, 2005). Values of S_s determined for five other aquifer tests to determine coal bed anisotropy in the PRB range from 2×10^{-5}/m to 1.6×10^{-4}/m. However, the Birney S_s value may be consistent with the low K_e value. The storage coefficient determined from the coal aquifer tests is that due mainly to the compressibility to the fracture pore space. The fracture pore space in this low-permeability coal is likely much smaller than that for most coals, and may be less compressible. The anisotropy ratio ($T_{\xi\xi}/T_{\eta\eta}$) of about 1.4 for this site is also somewhat smaller than those determined from other tests of PRB coals, which range from 1.8 to 2.9 (Weeks, 2005).

The horizontal head gradient in the Flowers-Goodale of about 3.1 m/km toward the NW is likely steeper and more westerly than the regional gradient, and is probably affected by the low permeability of the unit. On a regional scale, the permeability of the Flowers-Goodale is probably similar to that of typical PRB coal, or on the order of 100 times larger than was estimated here.

Typical MECoM technology would involve water pumped from the target coal, amended with nutrients, and re-injected (Ritter et al., 2015). It is assumed that re-injected fluid will remain in the coal aquifer for a few months before being pumped back. We had assumed that any reinjection would migrate for some distance, based on the combined effects of hydraulic gradient and aquifer anisotropy in the PRB. However, at the Birney test site, the water re-injected into the very low hydraulic conductivity Flowers-Goodale coal should migrate only a short distance in a few months. Thus, the effect of plume migration on pull-back of the re-injected nutrients and associated generated methane might not be significant, indicating this site might provide a more accurate quantitative estimate of local *in situ* CBM production compared to other sites with higher permeability. The slightly higher head in the well tapping the overlying sandstone is also encouraging, as the ambient downward gradient toward the Flowers-Goodale should prevent the injected fluid from migrating up into the overlying sandstone, despite the test-verified hydraulic connection between the two units.

3.4. Flowers-Goodale coal bed microbiology

Bioassays, in which a microbial consortium (WBC-2) was added to assess coal bioavailability, indicate that coal bioavailability was relatively low (0–3 μmol methane/g coal). There was increased methane production in coal from near the upper interface near the overlying sandstone indicating that the coal in this area of the coal bed was more bioavailable to WBC-2 (Fig. 7). In addition, of the 19 depths analyzed within the Flowers-Goodale coal bed, only one showed methane generation by the native microbial population, at the interface between the coal and an interbedded siltstone. Thus, while the conditions in the Flowers-Goodale are favorable for generation of biogenic methane, our preliminary analyses suggests that production could be improved by manipulating coal bioavailability, stimulating or amending the microbial population, or both. The potential to increase coal bioavailability makes the Flowers-Goodale an ideal test bed for developing methods for MECoM.

A total of 48,431 bacterial SSU-rRNA sequence reads were classified through pyrotag analysis after trimming and quality checking the sequences. The OTUs were defined with 3% dissimilarity and analyzed with Chao1 diversity estimates (Table S8) (Chao and Lee, 1992; Hughes et al., 2001). Chao1 statistics suggested further sequencing of the bacterial community would lead to additional OTUs and reveal more genera/species, but most of the bacterial diversity was accounted for with our analysis (Chao and Lee, 1992). Statistical analyses indicate the bacterial community detected in the drilling fluid grouped differently than the microbial communities detected from the center of the core samples (Fig. 8). These results suggest the drilling fluid used to obtain the cores did not contaminate the native community. The archaeal populations did not amplify indicating the methanogenic populations were below detection limits. Low archaeal abundance could explain why only one core sample produced measurable methane from the native population (Fig. 7). Sequences indicative of *Thermohydrogenium* were detected in many of the core samples, and *Thermohydrogenium* have been described as anaerobic, thermophilic fermentative bacteria (Fig. 8). Highly thermophilic microorganisms have previously been detected in cool environments such as the coal bed environment investigated here (Jones et al., 2013; Marchant et al., 2002). This microorganism has been used as a model hydrogen producer in anaerobic bioreactors (Teplyakov et al., 2002). Sequences related to *Aeribacillus*, commonly thought to be an aerobic microorganism, were also detected throughout the Flowers-Goodale coal seam especially near the upper interface near the sandstone overburden (Fig. 8) (Miñana-Galbis et al., 2010). Culturing results from the core samples indicate the Flowers-Goodale contains microbial communities capable of aerobic metabolism (Table S9). Researchers recently compared 160 microbial community compositions in ten hydrocarbon resource environments and sequenced twelve metagenomes to characterize their metabolic potential, and coal beds had unexpectedly high proportions of aerobic hydrocarbon-degrading bacteria (An et al., 2013), despite being highly reducing environments. An *Aeribacillus* spp. isolated from an oil-contaminated soil has recently been identified as a biosurfactant producer (Zheng et al., 2012). The production of biosurfactants could make the coal more bioavailable which could explain the higher methane production from WBC-2 near the sandstone overburden where *Aeribacillus* was most dominant.

Statistical analyses positively correlated *Actinobacteria* SSU-rRNA gene sequences with coal core samples rather than noncoal (clay or sand) cores (Fig. 9). *Actinobacteria* have been shown to play an important role in the decomposition of organic matter such as cellulose and chitin in peat bogs (Pankratov et al., 2006). Similarly to *Aeribacillus*, *Actinobacteria* have also been identified in oil reservoirs and the class *Actinomycetales* are associated with the production of biosurfactants that help solubilize and/or increase the bioavailability of hydrocarbons (Kügler et al., 2015). *Actinomycetales* spp. were detected in the coal at the interface near the overlying sandstone where *Aeribacillus* also dominated and methane production from WBC-2 was the greatest (Fig. 8).

The work presented here suggests bacteria capable of producing biosurfactants exist in coal beds and the production of biosurfactants may play an important role in the bioavailability of coal. Biosurfactants have previously been identified as emulsifying agents for hydrocarbons (Bognolo, 1999) and recent research indicated biosurfactant (rhamnolipid) production increased dramatically when coal was added to media containing a bacterium isolated from CBM water (Singh and Tripathi, 2013). In addition, biosurfactant production can be enhanced with the addition of nutrients such as yeast extract (Qazi et al., 2013). Yeast extract has been utilized in MECoM technology and has previously enhanced CBM production from microorganisms obtained from the PRB in laboratory studies (Barnhart et al., 2013; Green et al., 2008; Ritter et al., 2015). Future research should focus on the specific biosurfactants that are produced in coal beds and inexpensive

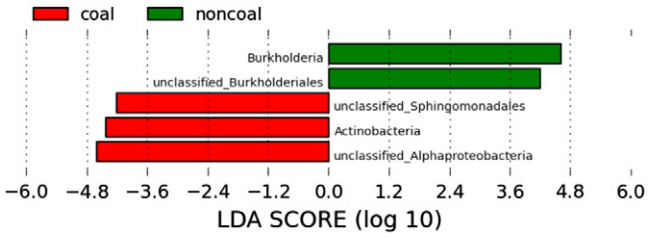

Fig. 9. LEfSe statistical analysis of the bacterial communities identified in coal samples and noncoal samples indicated that bacterial phylum *Actinobacteria* and unclassified *Sphingomonadales* and *Alphaproteobacteria* were associated with coal. The bacterial genus *Burkholderia* and unclassified *Burkholeriales* were more associated claystone and siltstone core samples.

nutrients that can be added to increase biosurfactant production. The application of technologies that increase biosurfactant production at the Birney test site and other coal beds could increase CBM production and help sustain the productive life of CBM wells. Results from this investigation might also be applied to other subsurface carbonaceous environments colonized by microbial communities because biogenic methane is present in black shale such as the New Albany and Antrim Shale, which contain biogenic methane associated with shale units of lower thermal maturity, similar to CBM (Martini et al., 1996; Schlegel et al., 2013; Strąpoć et al., 2010).

4. Summary and implications

The Birney test site was developed to better understand the hydrogeochemical and microbiological conditions that influence CBM production. Core desorption and water geochemistry analyses indicated the Flowers-Goodale and Terret coal beds contain biogenic methane and the extent of methanogenesis was greatest in the Flowers-Goodale coal bed. Aquifer-test results indicated the Flowers-Goodale coal bed at the Birney Test Site has very low hydraulic conductivity compared to other PRB coal beds examined. This low conductivity could be beneficial for MECoM tests because the nutrients should migrate slowly (0.005 m/d) from where they are injected which should allow time for microbial interaction. Local hydrology and hydrogeochemistry can differ from regional hydrology and this work highlights the importance of conducting a detailed hydrologic study before field studies can be undertaken and any planned MECoM technology can be implemented.

Bioassay methane production was greatest in coal samples from the upper interface of the Flowers-Goodale coal bed near the overlying sandstone. 454-pyrotag analysis identified sequences indicative of bacteria that could be biosurfactant producers in coal samples from the upper area of the coal bed where the bioassay methane production was the greatest. Biosurfactant production could have made the coal more bioavailable to the bioassay and suggests the addition of nutrients that enhance *in situ* biosurfactant production could increase bacterial coal degradation, the suspected rate-limiting step of coal-dependent methanogenesis. The described research provides novel insight into the *in situ* bacteria associated with coal and coal-interface material and potential pathways involved in coal degradation.

Acknowledgment

This work was supported by the U.S. Geological Survey Energy Resources Program. This material is based upon work supported by the Department of Energy under Award Number DE-FE0026155. This project was supported in part by DOE ZERT Program under grant no. DE-FC26-04NT42262. The development of pyrosequencing techniques was supported as a component of ENIGMA, a scientific focus area program supported by the U.S. Department of Energy, Office of Science, Office of Biological and Environmental Research, Genomics: GTL Foundational Science through contract DE-AC02-05CH11231 between Lawrence Berkeley National Laboratory and the U.S. Department of Energy. Research was also supported by a NSF grant (EAR-1322805).

Disclaimer: Any use of trade, firm, or product names is for descriptive purposes only and does not imply endorsement by the U.S. Government.

Appendix A. Supplementary data

Supplementary data to this article can be found online at http://dx.doi.org/10.1016/j.coal.2016.05.001.

References

Alfreider, A., Krossbacher, M., Psenner, R., 1997. Groundwater samples do not reflect bacterial densities and activity in subsurface systems. Water Res. 31, 832–840.

An, D., Caffrey, S.M., Soh, J., Agrawal, A., Brown, D., Budwill, K., Dong, X., Dunfield, P.F., Foght, J., Gieg, L.M., Hallam, S.J., Hanson, N.W., He, Z., Jack, T.R., Klassen, J., Konwar, K.M., Kuatsjah, E., Li, C., Larter, S., Leopatra, V., Nesbø, C.L., Oldenburg, T., Pagé, A.P., Ramos-Padron, E., Rochman, F.F., Saidi-Mehrabad, A., Sensen, C.W., Sipahimalani, P., Song, Y.C., Wilson, S., Wolbring, G., Wong, M.-L., Voordouw, G., 2013. Metagenomics of hydrocarbon resource environments indicates aerobic taxa and genes to be unexpectedly common. Environ. Sci. Technol. 47, 10708–10717.

Baker, G.C., Smith, J.J., Cowan, D.A., 2003. Review and re-analysis of domain-specific 16S primers. J. Microbiol. Methods 55, 541–555.

Bale, H.D., Carlson, M.L., Kalliat, M., Kwak, C.Y., Schmidt, P.W., 1984. Small-angle X-ray scattering of the submicroscopic porosity of some low-rank coals. In: Schobert, H.H. (Ed.), The Chemistry of Low-Rank Coals, pp. 79–94.

Barnhart, E.P., De Le'on, K.B., Ramsay, B.D., Cunningham, A.B., Fields, M.W., 2013. Investigation of coal-associated bacterial and archaeal populations from a diffusive microbial sampler (DMS). Int. J. Coal Geol. 115, 64–70.

Bates, B.L., McIntosh, J.C., Lohse, K.A., Brooks, P.D., 2011. Influence of groundwater flowpaths, residence times and nutrients on the extent of microbial methanogenesis in coal beds: Powder River Basin. USA Chem. Geol. 284, 45–61. http://dx.doi.org/10.1016/j.chemgeo.2011.02.004.

Blair, N., 1998. The δ^{13}C of biogenic methane in marine sediments: the influence of C(org) deposition rate. Chem. Geol. 152, 139–150. http://dx.doi.org/10.1016/S0009-2541(98)00102-8.

Bognolo, G., 1999. Biosurfactants as emulsifying agents for hydrocarbons. Colloids Surf. A Physicochem. Eng. Asp. 152, 41–52. http://dx.doi.org/10.1016/S0927-7757(98)00684-0.

Bowen De León, K., Gerlach, R., Peyton, B.M., Fields, M.W., 2013. Archaeal and bacterial communities in three alkaline hot springs in Heart Lake Geyser Basin, Yellowstone National Park. Front. Microbiol. 4, 330. http://dx.doi.org/10.3389/fmicb.2013.00330.

Bowen De León, K., Ramsay, B.D., Fields, M.W., 2012. Quality-score refinement of SSU rRNA gene pyrosequencing differs across gene region for environmental samples. Microb. Ecol. 64, 499–508. http://dx.doi.org/10.1007/s00248-012-0043-9.

Brinck, E.L., Drever, J.I., Frost, C.D., 2008. The geochemical evolution of water coproduced with coalbed natural gas in the Powder River Basin. Wyoming Environ. Geosci. 15, 153–171.

Capone, D.G., Kiene, R.P., 1988. Comparison of microbial dynamics in marine and freshwater sediments: contrasts in anaerobic carbon catabolism. Limnol. Oceanogr. 33, 725–749. http://dx.doi.org/10.4319/lo.1988.33.4_part_2.0725.

Chao, A., Lee, S.-M., 1992. Estimating the number of classes via sample coverage. J. Am. Stat. Assoc. 87, 210–217. http://dx.doi.org/10.2307/2290471.

Clark, L.D., Fritz, P., 1997. Environmental Isotopes in Hydrogeology. Lewis Publishers, New York.

Duffield, G.M., 2007. AQTESOLV™ for Windows, Version 4.1: HydroSOLV, Inc..

Ellis, M.S., Molnia, C.L., Osmonson, L.M., Ochs, A.M., Rohrbacher, T.J., Mercier, T., Roberts, N.R., 2002. Evaluation of economically extractable coal resouces in the gillete coal field. Power River Basin, Wyoming. U.S. Geological Survey Open-File Report 02–180.

Faison, B., 1992. The chemistry of low-rank coal and its relationship to the biochemical mechanisms of coal biotransformaiton, in: Crawford, D.L. (Ed. (Ed.), Microbial Transformations of Low Rank Coals. CRC Press, Inc., Boca Raton., pp. 1–26.

Faiz, M., Hendry, P., 2006. Significance of microbial activity in Australian coal bed methane reservoirs — a review. Bull. Can. Petrol. Geol. 54, 261–272. http://dx.doi.org/10.2113/gscpgbull.54.3.261.

Flores, R.M., Rice, C.A., Stricker, G.D., Warden, A., Ellis, M.S., 2008. Methanogenic pathways of coal-bed gas in the Powder River Basin, United States: the geologic factor. Int. J. Coal Geol. 76, 52–75. http://dx.doi.org/10.1016/j.coal.2008.02.005.

Formolo, M., Martini, A., Petsch, S., 2008. Biodegradation of sedimentary organic matter associated with coalbed methane in the Powder River and San Juan Basins, USA. Int. J. Coal Geol. 76, 86–97. http://dx.doi.org/10.1016/j.coal.2008.03.005.

Gieskes, J.M., Rogers, W.C., 1973. Alkalinity determination in interstitial waters of marine sediments. J. Sediment. Res. 43, 272–277. http://dx.doi.org/10.1306/74D72743-2B21-11D7-8648000102C1865D.

Gorody, A.W., 1999. The origin of natural gas in the tertiary coal seams on the eastern margin of the Powder River Basin. In: Miller, W.R. (Ed.), Coalbed Methane and the Tertiary Geology of the Powder River Basin, Wyoming and Montana; 50th Annual Field Conference Guidebook. Wyoming Geological Association, pp. 89–101.

Green, M.S., Flanegan, K.C., Gilcrease, P.C., 2008. Characterization of a methanogenic consortium enriched from a coalbed methane well in the Powder River Basin, U.S.A. Int. J. Coal Geol. 76, 34–45. http://dx.doi.org/10.1016/j.coal.2008.05.001.

Haas, B.J., Gevers, D., Earl, A.M., Feldgarden, M., Ward, D. V, Giannoukos, G., Ciulla, D., Tabbaa, D., Highlander, S.K., Sodergren, E., Methé, B., DeSantis, T.Z., Petrosino, J.F., Knight, R., Birren, B.W., 2011. Chimeric 16S rRNA sequence formation and detection in Sanger and 454-pyrosequenced PCR amplicons. Genome Res. 21, 494–504.

Holmes, C.W., Flores, R.M., Pocknall, D.T., 1991. Carbon isotopes in Tertiary coals of the Powder River Basin. J. Coal Qual. 10.

Hughes, J.B., Hellmann, J.J., Ricketts, T.H., Bohannan, B.J.M., 2001. Counting the uncountable: statistical approaches to estimating microbial diversity. Appl. Environ. Microbiol. 67, 4399–4406.

Jones, E.J.P., Harris, S.H., Barnhart, E.P., Orem, W.H., Clark, A.C., Corum, M.D., Kirshtein, J.D., Varonka, M.S., Voytek, M.A., 2013. The effect of coal bed dewatering and partial oxidation on biogenic methane potential. Int. J. Coal Geol. 115, 54–63.

Jones, E.J.P., Voytek, M.A., Corum, M.D., Orem, W.H., 2010. Stimulation of methane generation from nonproductive coal by addition of nutrients or a microbial consortium. Appl. Environ. Microbiol. 76, 7013–7022.

Jones, E.J.P., Voytek, M.A., Warwick, P.D., Corum, M.D., Cohn, A., Bunnell, J.E., Clark, A.C., Orem, W.H., 2008. Bioassay for estimating the biogenic methane-generating potential of coal samples. Int. J. Coal Geol. 76, 138–150. http://dx.doi.org/10.1016/j.coal.2008.05.011.

Klein, D.A., Flores, R.M., Venot, C., Gabbert, K., Schmidt, R., Stricker, G.D., Pruden, A., Mandernack, K., 2008. Molecular sequences derived from Paleocene Fort Union Formation coals vs. associated produced waters: implications for CBM regeneration. Int. J. Coal Geol. 76, 3–13. http://dx.doi.org/10.1016/j.coal.2008.05.023.

Kügler, J.H., Le Roes-Hill, M., Syldatk, C., Hausmann, R., 2015. Surfactants tailored by the class Actinobacteria. Front. Microbiol. 6. http://dx.doi.org/10.3389/fmicb.2015.00212.

Maasland, M., 1957. Soil anisotropy and land drainage, in Luthin (Ed.), Drainage of agricultural lands. Am. Soc. Agron. Monogr. 7, 226–227.

Marchant, R., Banat, I.M., Rahman, T.J., Berzano, M., 2002. The frequency and characteristics of highly thermophilic bacteria in cool soil environments. Environ. Microbiol. 4, 595–602. http://dx.doi.org/10.1046/j.1462-2920.2002.00344.x.

Martini, A.M.A., Budai, J.M.J., Walter, L.L.M., Schoell, M., 1996. Microbial generation of economic accumulations of methane within a shallow organic-rich shale. Nature 383, 155–157. http://dx.doi.org/10.1038/383155a0.

McIntosh, J.C., Martini, A.M., 2008. Hydrogeochemical indicators for microbial methane in fractured black shales: case studies of the Antrim, New Albany, and Ohio shales. In: Gas Shale in the Rocky Mountains and Beyond (Ed.), Rocky Mountain Association of Geologists 2008 Guidebook, pp. 162–174.

Meredith, E., Wheaton, J., Kuzara, S., 2012. Coalbed-methane basics ten years of lessons from the Powder River Basin. Mont. Bur. Mines Geol. Inf. Pam. 6.

Meslé, M., Dromart, G., Oger, P., 2013. Microbial methanogenesis in subsurface oil and coal. Res. Microbiol. 164, 959–972. http://dx.doi.org/10.1016/j.resmic.2013.07.004.

Miñana-Galbis, D., Pinzón, D.L., Lorén, J.G., Manresa, À., Oliart-Ros, R.M., 2010. Reclassification of Geobacillus pallidus (Scholz et al. 1988) Banat et al. 2004 as Aeribacillus pallidus gen. nov., comb. nov. Int. J. Syst. Evol. Microbiol. 60, 1600–1604. http://dx.doi.org/10.1099/ijs.0.003699-0.

Moench, A.F., 1985. Transient flow to a large-diameter well in an aquifer with storative semiconfining layers. Water Resour. Res. 21, 1121–1131.

Moench, A.F., 1984. Double-porosity models for a fissured groundwater reservoir with fracture skin. Water Resour. Res. 20, 831–846.

Molnia, C.L., Pierce, F.W., 1992. Cross Sections Showing Coal Stratigraphy of the Central Powder River Basin, Wyoming and Montana: U.S. Geological Survey Miscellaneous Investigations Series Map I-1959-D, 1 sheet (scale 1:500,000).

Orem, W., Tatu, C., Varonka, M., Lerch, H., Bates, A., Engle, M., Crosby, L., McIntosh, J., 2014. Organic substances in produced and formation water from unconventional natural gas extraction in coal and shale. Int. J. Coal Geol. 126, 20–31.

Orem, W.H., Tatu, C.A., Lerch, H.E., Rice, C.A., Bartos, T.T., Bates, A.L., Tewalt, S., Corum, M.D., 2007. Organic compounds in produced waters from coalbed natural gas wells in the Powder River Basin, Wyoming, USA. Appl. Geochem. 22, 2240–2256. http://dx.doi.org/10.1016/j.apgeochem.2007.04.010.

Osborn, S.G., McIntosh, J.C., 2010. Chemical and isotopic tracers of the contribution of microbial gas in Devonian organic-rich shales and reservoir sandstones, northern Appalachian Basin. Appl. Geochem. 25, 456–471. http://dx.doi.org/10.1016/j.apgeochem.2010.01.001.

Palmer, I., 2010. Coalbed methane completions: a world view. Int. J. Coal Geol. 82, 184–195.

Pankratov, T.A., Dedysh, S.N., Zavarzin, G.A., 2006. The leading role of actinobacteria in aerobic cellulose degradation in Sphagnum peat bogs. Microbiology 410, 428–430.

Papadopulos, I.S., 1965. Non-steady Flow to a Well in an Infinite Anisotropic Aquifer, in: International Association of Scientific Hydrology Symposium. Dubrovnik, Yugoslavia, pp. 21–31.

Qazi, M.A., Malik, Z.A., Qureshi, G.D., Hameed, A., Ahmed, S., 2013. Yeast extract as the most preferable substrate for optimized biosurfactant production by rhlb gene positive pseudomonas putida sol- 10 isolate. J. Biorem. Biodegrad. 4, 204. http://dx.doi.org/10.4172/2155-6199.1000204.

Raskin, L., Rittmann, B.E., Stahl, D.A., 1996. Competition and coexistence of sulfate-reducing and methanogenic populations in anaerobic biofilms. Appl. Environ. Microbiol. 62, 3847–3857.

Rehm, B.W., Groenewold, G.H., Morin, K.A., 1980. Hydraulic properties of coal and related materials, Northern Great Plains. Ground Water 18, 551–561.

Rice, C.A., Flores, R.M., Stricker, G.D., Ellis, M.S., 2008. Chemical and stable isotopic evidence for water/rock interaction and biogenic origin of coalbed methane, Fort Union Formation, Powder River Basin, Wyoming and Montana U.S.A. Int. J. Coal Geol. 76, 76–85. http://dx.doi.org/10.1016/j.coal.2008.05.002.

Ritter, D., Vinson, D., Barnhart, E.P., Akob, D., Fields, M.W., Cunningham, A.B., Orem, W.H., McIntosh, J.C., 2015. Enhanced microbial coalbed methane generation: a review of research, commercial activity, and remaining challenges. Int. J. Coal Geol. 146 (1), 28–41. http://dx.doi.org/10.1016/j.coal.2015.04.013.

Rouquerolt, J., Avnir, D., Fairbridge, C.W., Everett, D.H., Haynes, J.H., Pernicone, N., Ramsay, J.D.F., Sing, K.S.W., Unger, K.K., 1994. Recommendations for the characterization of porous solids. Pure Appl. Chem. 66, 1739–1758. http://dx.doi.org/10.1351/pac199466081739.

Sando, S.K., Vecchia, A.V., Barnhart, E.P., Sando, T.R., Clark, M.L., Lorenz, D.L., 2014. Trends in Major-ion Constituents and Properties for Selected Sampling Sites in the Tongue and Powder River Watersheds, Montana and Wyoming, Based on Data Collected During Water Years 1980–2010: U.S. Geological Survey Scientific Investigations Report 2013-5179.

Schlegel, M.E., McIntosh, J.C., Petsch, S.T., Orem, W.H., Jones, E.J.P., Martini, A.M., 2013. Extent and limits of biodegradation by in situ methanogenic consortia in shale and formation fluids. Appl. Geochem. 28, 172–184.

Scott, D.C., Haacke, J.E., Osmonson, L.M., Luppens, J.A., Pierce, P.E., Rohrbacher, T.J., 2011. Assessment of Coal Geology, Resources, and Reserves in the Northern Wyoming Powder River Basin: U.S. Geological Survey Open-File Report 2010–1294.

Segata, N., Izard, J., Waldron, L., Gevers, D., Miropolsky, L., Garrett, W.S., Huttenhower, C., 2011. Metagenomic biomarker discovery and explanation. Genome Biol. 12, R60.

Singh, D.N., Tripathi, A.K., 2013. Coal induced production of a rhamnolipid biosurfactant by Pseudomonas stutzeri, isolated from the formation water of Jharia coalbed. Bioresour. Technol. 128, 215–221. http://dx.doi.org/10.1016/j.biortech.2012.10.127.

Strąpoć, D., Mastalerz, M., Dawson, K., Macalady, J., Callaghan, A. V, Wawrik, B., Turich, C., Ashby, M., 2011. Biogeochemistry of microbial coal-bed methane. Annu. Rev. Earth Planet. Sci. 39, 617–656. doi:http://dx.doi.org/10.1146/annurev-earth-040610-133343

Strąpoć, D., Mastalerz, M., Schimmelmann, A., Drobniak, A., Hasenmueller, N.R., 2010. Geochemical constraints on the origin and volume of gas in the New Albany Shale (Devonian-Mississippian), eastern Illinois Basin. Am. Assoc. Pet. Geol. Bull. 94, 1713–1740.

Strąpoć, D., Picardal, F.W., Turich, C., Schaperdoth, I., Macalady, J.L., Lipp, J.S., Lin, Y.-S., Ertefai, T.F., Schubotz, F., Hinrichs, K.-U., Mastalerz, M., Schimmelmann, A., 2008. Methane-producing microbial community in a coal bed of the Illinois Basin. Appl. Environ. Microbiol. 74, 2424–2432.

Teplyakov, V.V., Gassanova, L.G., Sostina, E.G., Slepova, E.V., Modigell, M., Netrusov, A.I., 2002. Lab-scale bioreactor integrated with active membrane system for hydrogen production: experience and prospects. Int. J. Hydrog. Energy 27, 1149–1155. http://dx.doi.org/10.1016/S0360-3199(02)00093-9.

U.S. Geological Survey National Assessment of Oil and Gas Resources Team, Biewick, L.R.H., compiler, 2014. Map of Assessed Coalbed-Gas Resources in the United States, 2014: U.S. Geological Survey Digital Data Series 69–II. doi: http://dx.doi.org/10.3133/ds69ii

Ulrich, G., Bower, S., 2008. Active methanogenesis and acetate utilization in Powder River Basin coals, United States. Int. J. Coal Geol. 76, 25–33.

Wawrik, B., Mendivelso, M., Parisi, V., Suflita, J., Davidova, I., Marks, C., Nostrand, J., Liang, Y., Zhou, J., Huizinga, B., Strapoc, D., Callaghan, A. V, 2011. Field and laboratory studies on the bioconversion of coal to methane in the San Juan Basin. Fems Micriobiology Ecol. 81, 26–42.

Weeks, E.P., 2005. Hydrologic properties of coal-beds in the Powder River Basin, Montana. II. Aquifer test analysis. J. Hydrol. 308, 242–257.

Whiticar, M., Faber, E., Schoell, M., 1986. Biogenic methane formation in marine and freshwater environments: CO2 reduction vs. acetate fermentation—isotope evidence. Geochim. Cosmochim. Acta 50, 693–709. http://dx.doi.org/10.1016/0016-7037(86)90346-7.

Whiticar, M.J., 1999. Carbon and hydrogen isotope systematics of bacterial formation and oxidation of methane. Chem. Geol. 161, 291–314. http://dx.doi.org/10.1016/S0009-2541(99)00092-3.

Yakimov, M.M., Giuliano, L., Chernikova, T.N., Gentile, G., Abraham, W.R., Lunsdorf, H., Timmis, K.N., Golyshin, P.N., 2001. Alcalilimnicola halodurans gen. nov., sp nov., an alkaliphilic, moderately halophilic and extremely halotolerant bacterium, isolated from sediments of soda-depositing Lake Natron, East Africa Rift Valley. Int. J. Syst. Evol. Microbiol. 51, 2133–2143.

Yoder, J., 2013. Making Heatmaps with R for Microbiome Analysis [WWW Document]. Mol. Ecol. URL http://www.molecularecologist.com/2013/08/making-heatmaps-with-r-for-microbiome-analysis/

Zheng, C., Li, Z., Su, J., Zhang, R., Liu, C., Zhao, M., 2012. Characterization and emulsifying property of a novel bioemulsifier by Aeribacillus pallidus YM-1. J. Appl. Microbiol. 113, 44–51.